Acta Cryst. (1988). C**44**, 400–405

$Y_4Ir_9Si_5$, a New Substitution Variant of the Ce_2Ni_7 Type and Isotypes of Other Members of the $R_{2+n}T_{3+3n}M_{1+2n}$ Structure Series

BY K. CENZUAL, B. CHABOT AND E. PARTHÉ

Laboratoire de Cristallographie aux Rayons X, Université de Genève, 24, Quai Ernest Ansermet, CH-1211 Geneva 4, Switzerland

(*Received* 1 *October* 1987; *accepted* 10 *November* 1987)

Abstract. $Y_4Ir_{9+x}Si_{5-x}$, $x = 0{\cdot}12$ (2), $M_r = 2226$ for $Y_4Ir_9Si_5$, *hP*36, $P6_3/mmc$, $a = 5{\cdot}4894$ (2), $c = 22{\cdot}6054$ (9) Å, $V = 589{\cdot}93$ (6) Å^3, $Z = 2$, $D_x = 12{\cdot}53$ Mg m^{-3} ($Y_4Ir_9Si_5$), Mo $K\alpha$, $\lambda = 0{\cdot}71073$ Å, $\mu = 127{\cdot}4$ mm^{-1}, $F(000) = 1838$, $T = 293$ K, $wR = 0{\cdot}061$ for 308 independent reflections. The $Y_4Ir_9Si_5$ type is a site-occupation variant of the Ce_2Ni_7 type. It is a new member ($n = 2$) of the hexagonal branch of the structure series $R_{2+n}T_{3+3n}M_{1+2n}$, grouping types where ternary Laves-type slabs are intergrown with ternary $CeCo_3B_2$-type slabs. $ErRh_2Si$, $ErRh_2Ge$, YIr_2Si and YRh_2Ge were found to crystallize with the YRh_2Si type (site-occupation variant of the $CeNi_3$ type), $Er_4Rh_9Ge_5$ and $Y_4Rh_9Ge_5$ with the $Y_4Rh_9Si_5$ type (site-occupation variant of the Gd_2Co_7 type). The former structure type belongs to the hexagonal and the latter to the rhombohedral branch of the same structure series.

Introduction. The well known Laves types and the $CaCu_5$ type are widely spread among binary compounds. In several R–T systems (R = rare-earth element, T = transition metal), structures where one Laves-type slab (R_2T_4) is intergrown with n $CaCu_5$-type slabs (RT_5) have been found at intermediate compositions. The $R_{2+n}T_{4+5n}$ structure series grouping these structures can be subdivided into two branches depending on the stacking of the Laves-type slabs. In the rhombohedral branch the Laves-type slabs are stacked as in the cubic Laves-type $MgCu_2$ and in the hexagonal branch the same slabs are stacked as in the hexagonal $MgZn_2$ type (Parthé & Lemaire, 1975). Simple ordered substitution variants with composition R_2T_3M (M = main-group element) are known for both Laves types: Mg_2Cu_3Si (Witte, 1939) with $MgZn_2$-type stacking and Mg_2Ni_3Si (Noréus, Eriksson, Göthe & Werner, 1985) or Y_2Rh_3Ge (Cenzual, Chabot & Parthé, 1987) with $MgCu_2$-type stacking. $CeCo_3B_2$ (Kuz'ma, Kripyakevich & Bilonizhko, 1969) is a ternary ordered substitution variant of $CaCu_5$ with composition RT_3M_2. Three ternary structure series can then be imagined where one or both kinds of slabs are ternary. The members of these series are substitution variants of the members of the binary $R_{2+n}T_{4+5n}$ structure series. In reality, several borides have been found to crystallize with structures where binary Laves-type slabs are intergrown with ternary $CeCo_3B_2$-type slabs (Kuz'ma, 1979; Kuz'ma & Chaban, 1980) and one silicide and several aluminides (see Parthé & Chabot, 1984) have been reported to crystallize with a structure type where a ternary Laves-type slab is intergrown with a binary $CaCu_5$-type slab (Bodak, 1971). Two structures belonging to the structure series $R_{2+n}T_{3+3n}M_{1+2n}$ where both kinds of slabs are ternary were recently found in the Y–Rh–Si system (Paccard, Paccard, Moreau & Gomez-Sal, 1985; Paccard & Paccard, 1985). We decided to look for structures belonging to the same series in other systems with silicon or germanium in order to see if a ternary stacking variant was formed and, in that case, which one of the two possible stackings of the Laves-type slabs was observed.

Experimental.

Structure determination and refinement of $Y_4Ir_{9+x}Si_{5-x}$

Sample of nominal composition $Y_4Ir_9Si_5$ (Y 99·5, Ir 99·9, Ge 99·999%), prepared in an arc furnace under purified Ar atmosphere, annealed at 1273 K for 7 d and further remelted by levitation techniques and slowly cooled down to room temperature. The comparison between the powder X-ray diffraction diagram (Guinier–Nonius camera) with theoretical powder diagrams, calculated with the program *LAZY PULVERIX* (Yvon, Jeitschko & Parthé, 1977), suggested a structure related to the Ce_2Ni_7 type (Cromer & Larson, 1959). Crystal of irregular shape (mean radius 50 μm); Philips PW 1100 four-circle diffractometer; graphite-monochromated Mo $K\alpha$ radiation. Cell parameters refined from 2θ values of 12 reflections (Mo $K\alpha_1$, $\lambda = 0{\cdot}70930$ Å; $49 \le 2\theta \le 60°$) using the program *FINAX* (Hovestreydt, 1983). Laue symmetry 6/*mmm*; possible space groups $P6_3mc$, $P\bar{6}2c$ and $P6_3/mmc$ when admitting systematic absences hhl $l \neq 2n$. 719 reflections collected out to $(\sin\theta)/\lambda = 0{\cdot}70$ Å^{-1} ($0 \le h,k \le 7$; $0 \le l \le 31$) in the ω–2θ scan mode, yielding 387 independent reflections ($R_{int} = 0{\cdot}14$), of which 257 were considered significant [$|I| \ge 3\sigma(I)$]. Standard reflections 017 and 107 (max. intensity variation ±2·7%); spherical absorption correction ($\mu R = 6{\cdot}4$; $62{\cdot}4 \le A^* \le 317{\cdot}7$). The high values of the absorption

0108-2701/88/030400-06$03.00

coefficients explain the large differences between symmetry-equivalent reflections while applying a spherical absorption correction. Full-matrix refinement in $P6_3/mmc$ from the coordinates of Ce_2Ni_7, using $|F|$ values of 308 independent reflections (including 53 less-thans calculated greater than observed and ignoring the reflections 006 and 0,0,12, strongly affected by absorption and extinction). 7 positional parameters and 6 isotropic displacement parameters, listed in Table 1, one occupation factor and one scale factor refined to a final $wR = 0{\cdot}061$ [$w = 1/\sigma^2(|F_{rel}|)$; $S = 4{\cdot}31$; shift/e.s.d. in the last cycle $\leq 0{\cdot}0002$; max. (min.) height of final residual electron density map = 6·5 (−7·8) e Å^{-3}].* Interatomic distances out to 3·6 Å are listed in Table 2. Atomic scattering factors for neutral atoms, f' and f'' from *International Tables for X-ray Crystallography* (1974); programs used for data reduction and structure refinement from the *XRAY*76 system (Stewart, Machin, Dickinson, Ammon, Heck & Flack, 1976).

A mixed occupation of Si and Ir was refined at site Si(3) since the isotropic displacement parameter for this site was negative for $PP(Si) = 1$. Because of the high correlation between the isotropic displacement parameter and the population parameter the former was fixed at 0·008 Å^2 in the final refinement. With the assumption of a fully occupied site a population of 88 (2)% Si–12% Ir was found. The sample, which was prepared at the nominal composition 4–9–5, contained several phases even after annealing for 7 d at 1273 K. We do not know whether the composition corresponding to $x = 0$ is included in the homogeneity range of the Ce_2Ni_7 substitution variant in this system; however, the structure will from here on be referred to as the $Y_4Ir_9Si_5$ type.

New compounds crystallizing with the YRh_2Si *and* $Y_4Rh_9Si_5$ *types*

Compounds crystallizing with one of the structure types belonging to the $R_{2+n}T_{3+3n}M_{1+2n}$ structure series were looked for in the following systems: Y–Co–Si, Y–Ni–Si, Y–Ru–Si, Y–Rh–Ge, Er–Rh–Si, Er–Rh–Ge, Y–Ir–Si, Y–Ir–Ge. Samples of composition 1–2–1 ($n = 1$), in some systems also 4–9–5 ($n = 2$) and 5–12–7 ($n = 3$), were prepared in the arc furnace, wrapped in Ta foil and annealed for 7 d at 1273 K (1073 K for Co- or Ni-containing alloys) in sealed quartz tubes under Ar atmosphere. Powder X-ray diffraction films (Guinier–Nonius camera) of as-cast and annealed samples were compared with the diffraction patterns calculated with the program *LAZY PULVERIX*. YRh_2Ge, $ErRh_2Si$, $ErRh_2Ge$ and YIr_2Si were found to crystallize with the YRh_2Si type, *hP*24, $P6_3/mmc$ (Paccard & Paccard, 1985) and $Y_4Rh_9Ge_5$, $Er_4Rh_9Si_5$ and $Er_4Rh_9Ge_5$ with the $Y_4Rh_9Si_5$ type, *hR*54, $R\bar{3}m$ (Paccard, Paccard, Moreau & Gomez-Sal, 1985). The lattice parameters, given in Table 3, were refined from the 2θ values of 20–25 reflections measured on the films of the annealed samples [Cu $K\alpha$, $\lambda = 1{\cdot}54184$ Å; $18 \leq 2\theta \leq 75°$; internal standard Si ($a = 5{\cdot}4307$ Å)], using the program *FINAX* (Hovestreydt, 1983). In the case of $Er_4Rh_9Si_5$ a slight line splitting was observed which has not been taken into account for the determination of the approximate cell.

Table 1. *Atomic coordinates and isotropic displacement parameters for* $Y_4Ir_{9+x}Si_{5-x}$ *with space group* $P6_3/mmc$

The temperature factor is expressed as $T = \exp\{-2\pi^2 U[2(\sin\theta)/\lambda]^2\}$. E.s.d.'s are given in parentheses.

		x	y	z	100 U(Å^2)
Ir(1)	12(k)	0·1674 (3)	2x	0·0880 (1)	0·6 (1)
Ir(2)	6(h)	0·1663 (6)	2x	¼	0·7 (1)
Si(1)	4(f)	⅓	⅔	0·1681 (14)	1·4 (4)
Y(1)	4(f)	⅓	⅔	0·5277 (3)	0·5 (1)
Y(2)	4(f)	⅓	⅔	0·6737 (4)	1·0 (1)
Si(2)	4(e)	0	0	0·1670 (15)	1·1 (5)
Si(3)*	2(a)	0	0	0	0·8

* Mixed occupation Si–Ir, $PP(Si) = 0{\cdot}88$ (2) when the constraint $PP(Si) + PP(Ir) = 1$ is applied.

Table 2. *Interatomic distances* (d) *out to* 3·6 Å *and* $\Delta = (d - \sum r)/\sum r$ *for* $Y_4Ir_9Si_5$; *e.s.d.'s are given in parentheses*

Atomic radii (r) used are 1·801 (Y), 1·357 (Ir) and 1·319 Å (Si) respectively (Teatum, Gschneidner & Waber, 1960).

		d(Å)	Δ(%)
Y(1)–	3Ir(1)	3·054 (7)	−3·3
	6Ir(1)	3·064 (4)	−3·0
	3Si(3)	3·230 (2)	+3·5
	Y(2)	3·300 (12)	−8·4
	3Y(1)	3·408 (4)	−5·4
Y(2)–	3Si(1)	3·172 (1)	+1·7
	3Si(2)	3·173 (2)	+1·7
	6Ir(2)	3·242 (6)	+2·7
	Y(1)	3·300 (12)	−8·4
	6Ir(1)	3·360 (6)	+6·4
	Y(2)	3·451 (13)	−4·2
Ir(1)–	Si(2)	2·393 (25)	−10·6
	Si(1)	2·403 (23)	−10·2
	Si(3)	2·547 (1)	−4·8
	2Ir(1)	2·733 (1)	+0·7
	2Ir(1)	2·756 (1)	+1·6
	Y(1)	3·054 (7)	−3·3
	2Y(1)	3·064 (4)	−3·0
	2Y(2)	3·360 (6)	+6·4
Ir(2)–	2Si(1)	2·439 (23)	−8·9
	2Si(2)	2·453 (26)	−8·3
	2Ir(2)	2·739 (2)	+0·9
	2Ir(2)	2·750 (2)	+1·3
	4Y(2)	3·242 (6)	+2·7
Si(1)–	3Ir(1)	2·403 (23)	−10·2
	3Ir(2)	2·439 (23)	−8·9
	3Si(2)	3·169 (1)	+20·1
	3Y(2)	3·172 (1)	+1·7
Si(2)–	3Ir(1)	2·393 (25)	−10·6
	3Ir(2)	2·453 (26)	−8·3
	3Si(1)	3·169 (1)	+20·1
	3Y(2)	3·173 (2)	+1·7
Si(3)–	6Ir(1)	2·547 (1)	−4·8
	6Y(1)	3·230 (2)	+3·5

Discussion.

The structure of $Y_4Ir_9Si_5$

$Y_4Ir_{9+x}Si_{5-x}$ is a substitution variant of the binary Ce_2Ni_7 type, *hP*36, $P6_3/mmc$ (Cromer & Larson, 1959) and, if $x = 0$, a member of the hexagonal branch of the

* Lists of structure factors arranged in a standard crystallographic data file (Brown, 1985) have been deposited with the British Library Document Supply Centre as Supplementary Publication No. SUP 44532 (11 pp.). Copies may be obtained through The Executive Secretary, International Union of Crystallography, 5 Abbey Square, Chester CH1 2HU, England.

Table 3. *The occurrence of structure types containing intergrown Laves-type and/or* $CaCu_5$*-type slabs in the* Y–Rh, Er–Rh *and* Y–Ir *systems and corresponding ternary systems with* Si *and* Ge

Compounds identified in this work are written with bold letters. r = rhombohedral branch, h = hexagonal branch. For compounds crystallizing with the cubic $MgCu_2$ type (as well as for all rhombohedral structures), the parameters of the triple hexagonal cell are given.

n	Compound	Type	Branch	a(Å)	c(Å)	Compound	Type	Branch	a(Å)	c(Å)	Compound	Type	Branch	a(Å)	c(Å)
	Y–Rh					Y–Rh–Si					Y–Rh–Ge				
0	YRh_2[a]	$MgCu_2$	r	5·302	12·99	Not observed					Y_2Rh_3Ge[e]	Mg_2Ni_3Si	r	5·552 (3)	11·82 (1)
1	YRh_3[a]	$CeNi_3$	h	5·230	17·38	YRh_3Si[b]	YRh_2Si	h	5·495 (2)	15·030 (5)	YRh_3Ge	YRh_2Si	h	**5·520 (1)**	**15·50 (2)**
2	Not observed					$Y_4Rh_5Si_5$[c]	$Y_4Rh_9Si_5$	r	5·496 (1)	33·176 (8)	$Y_4Rh_9Ge_5$	$Y_4Rh_9Si_5$	r	**5·523 (1)**	**34·54 (1)**
∞	YRh_5[a]	$CaCu_5$		5·141	4·294	YRh_3Si_2[d]	$ErRh_3Si_2$*								
	Er–Rh					Er–Rh–Si					Er–Rh–Ge				
0	$ErRh_2$[f]	$MgCu_2$	r	5·263	12·89	Er_2Rh_3Si[e]	Mg_2Ni_3Si	r	5·500 (1)	11·562 (3)	Er_2Rh_3Ge[e]	Mg_2Ni_3Si	r	5·523 (1)	11·762 (3)
1	Not observed					$ErRh_2Si$	YRh_2Si	h	**5·480 (1)**	**14·977 (3)**	$ErRh_2Ge$	YRh_2Si	h	**5·499 (1)**	**15·433 (3)**
2	Not observed					$Er_4Rh_9Si_5$	$Y_4Rh_9Si_5$	r	≃ 5·49	≃ 33·1†	$Er_4Rh_9Ge_5$	$Y_4Rh_9Si_5$	r	**5·501 (1)**	**34·427 (7)**
∞	$ErRh_5$[c]	$CaCu_5$		5·118	4·292	$ErRh_3Si_2$[d]	$ErRh_3Si_2$*								
	Y–Ir					Y–Ir–Si					Y–Ir–Ge				
0	YIr_2[h]	$MgCu_2$	r	5·321	13·03	Not observed					Not observed				
1	YIr_3[i]	$PuNi_3$	r	5·274	26·043	YIr_2Si	YRh_2Si	h	**5·488 (1)**	**15·281 (4)**	Not observed				
2	Not observed					$Y_4Ir_9Si_5$	$Y_4Ir_9Si_5$	h	**5·489 (1)**	**22·605 (1)**	Not observed				
∞	Not observed					Not observed									

References: (*a*) Ghassem & Raman (1973*a*); (*b*) Paccard & Paccard (1985); (*c*) Paccard, Paccard, Moreau & Gomez-Sal (1985); (*d*) Cenzual, Chabot & Parthé (1988); (*e*) Cenzual, Chabot & Parthé (1987); (*f*) Ghassem & Raman (1973*b*); (*g*) Raman & Ghassem (1973); (*h*) Krikorian (1971); (*i*) Fradin, Radousky, Zaluzec, Knapp & Downey (1982). For literature references of less-recent structure types see Villars & Calvert (1985).

* Orthorhombic deformation superstructure of the $CeCo_3B_2$ type.
† Approximate parameters.

ternary structure series $R_{2+n}T_{3+3n}M_{1+2n}$ with $n = 2$. Another substitution variant of Ce_2Ni_7, where a binary Laves-type slab is intergrown with two ternary $CeCo_3B_2$-type slabs, has been identified for $Ce_2Co_5B_2$ (Kuz'ma, 1979). For this particular ordering variant $x = 1$.

The structure of $Y_4Ir_9Si_5$ is shown in a projection along a short orthohexagonal axis in Fig. 1. Dashed lines delimit the Laves-type (labelled Mg_2Cu_3Si) and $CeCo_3B_2$-type slabs. The interface between the slabs is formed by a Kagomé net of Ir atoms whereas the Si sites are located inside the slabs. The Si(3) site, for which substitution of Si by Ir was observed, belongs to the Laves-type slab. One slight deformation from the binary model can be seen from the drawing: the Y atoms of the $CeCo_3B_2$-type slab are not in the bisecting plane of the slab but slightly displaced (0·1 Å) towards the neighbouring $CeCo_3B_2$-type slab.

The interatomic distances out to 3·6 Å and their relative contraction as compared with the sum of the radii of 12-coordinated atoms (Teatum, Gschneidner & Waber, 1960) are listed in Table 2. As expected, important contractions are observed in the distances between Ir and Si. However, the structures belonging to the ternary subseries where one Laves-type slab is intergrown with n $CeCo_3B_2$ slabs are also characterized by short R–R distances. The Y(1) site which is inside the Laves-type slab is surrounded by a tetrahedron of Y atoms at short distances ($1 \times \Delta = -8{\cdot}4$, $3 \times \Delta = -5{\cdot}4\%$) as in the Laves-type phases themselves, while the Y(2) site inside the $CeCo_3B_2$-type slab has short distances to two Y atoms ($\Delta = -8{\cdot}4$ and $-4{\cdot}2\%$) along

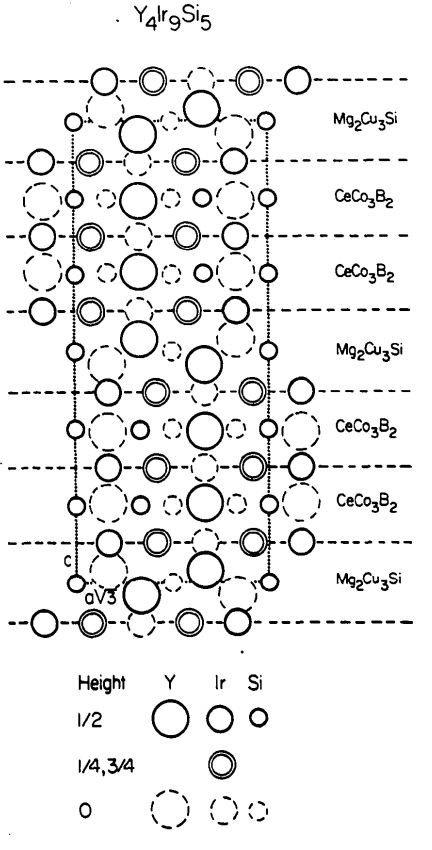

Fig. 1. The structure of $Y_4Ir_9Si_5$ in a projection along [110]. Dashed lines indicate the interfaces between ternary Laves- and $CeCo_3B_2$-type slabs.

the c axis, as in $CeCo_3B_2$. A three-dimensional network of Y atoms is thus observed throughout the structure. If the Y(2) atoms were in the bisecting plane of the slab an even more important contraction would be observed in the distance between Y(1) and Y(2).

Laves – $CaCu_5$ structure series

In Fig. 2(*a*) are presented the compositions of the structure types belonging to one of the four structure series where one binary or ternary Laves-type slab is intergrown with n binary or ternary $CaCu_5$-type slabs. Above the general formulae of the structure series are shown two partial triangular R–T–M composition diagrams on which are indicated the structure types of those series which have been identified at present. Heavy lines connect the structures where $n = 0$ and $n = \infty$ respectively. On the upper diagram are indicated those structure types where the Laves-type slabs are stacked as in $MgZn_2$ or its ternary substitution variant Mg_2Cu_3Si – hexagonal branches – and on the lower one

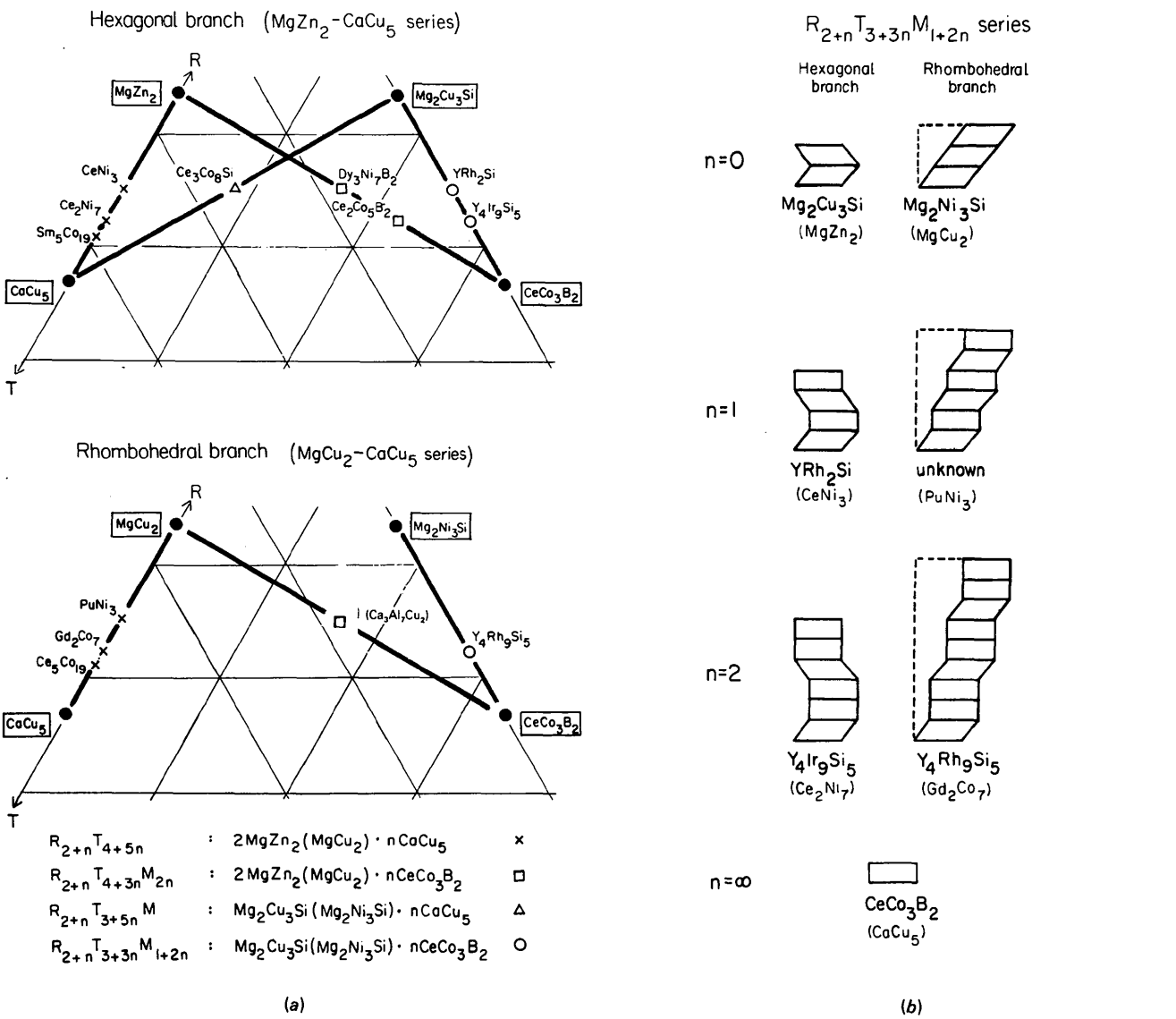

Fig. 2. (*a*) Compositions of the different structure types where one binary or ternary Laves-type slab is intergrown with n binary or ternary $CaCu_5$-type slabs. Above the general formulae of the structure series are shown two partial triangular R–T–M composition diagrams. In the structure types indicated, in the upper one the Laves-type slabs are stacked as in $MgZn_2$ (hexagonal branch) whereas in the lower one the same slabs are stacked as in $MgCu_2$ (rhombohedral branch). Formula in parentheses indicates that T and M sites are interchanged. (*b*) Schematic drawings of the members of the $R_{2+n}T_{3+3n}M_{1+2n}$ structure series. Corresponding binary structure types are indicated in parentheses. Rhombs correspond to the repetition unit of the Laves-type slabs of composition R_2T_3M and rectangles to the repetition unit of the $CaCu_5$-type slabs of composition RT_3M_2. Literature references for less-recent structure types may be found in Villars & Calvert (1985).

the structures where the stacking of the same slabs is similar to that observed in $MgCu_2$ or Mg_2Ni_3Si – rhombohedral branches. It may be noticed that no intergrowth structures are known where the number of Laves-type slabs exceeds the number of $CaCu_5$-type slabs.

Structure types where only the $CaCu_5$-type slabs contain M atoms ($R_{2+n}T_{4+3n}M_{2n}$ series) have been identified for a number of R–T borides where T = Co or Ni. A point has also been included for a rhombohedral $R_3T_7M_2$ compound of this series which is found with $Ca_3Al_7Cu_2$ (Cordier, Czech, Ochmann & Schäfer, 1984) where Al occupies T and Cu M sites. The structure type containing alternate ternary Laves- and binary $CaCu_5$-type slabs ($R_{2+n}T_{3+5n}M$ series) was first identified with Ce_3Co_8Si but has also been observed with aluminides (T = Ni).

Schematic drawings of the structure types belonging to the $R_{2+n}T_{3+3n}M_{1+2n}$ structure series where both kinds of slabs contain M atoms are shown in Fig. 2(*b*). The subsitution variant of the rhombohedral $PuNi_3$ type (also called Be_3Nb type) with composition RT_2M has not yet been observed. The compounds, characterized at present, which crystallize with one of the structure types of the $R_{2+n}T_{3+3n}M_{1+2n}$ series are listed in Table 3 together with the compounds reported in the corresponding binary systems which belong to the $R_{2+n}T_{4+5n}$ series. No ternary types belonging to this structure family were observed in the Y–Ir–Ge system.

While YRh_5 and $ErRh_5$ have been reported with the $CaCu_5$ type, the corresponding ternary silicides crystallize with the $ErRh_3Si_2$ type (Cenzual, Chabot & Parthé, 1988), an orthorhombic deformation variant of $CeCo_3B_2$ where $a \simeq 2c(CeCo_3B_2)$, $b \simeq 3^{1/2}a(CeCo_3B_2)$ and $c \simeq a(CeCo_3B_2)$. In $ErRh_3Si_2$ the columns of rare-earth atoms parallel to the pseudo-hexagonal axis are not straight as in the $CeCo_3B_2$ type but zigzagged. A related deformation may be present in the structure of $Er_4Rh_9Si_5$ containing two successive $CeCo_3B_2$-type slabs since a slight line splitting is observed on powder X-ray diffraction films.

Stacking of the Laves-type slabs

Whereas, especially with the silicides, compounds with various n values were often present simultaneously in a sample with 'stoichiometric' composition, only one stacking variant was observed for each value of n. For the group of compounds studied here the change from Y to Er does not affect the stacking mode of successive Laves-type slabs, separated or not by intermediate $CaCu_5$-type slabs. The substitution of Si by Ge modifies the conditions for the existence of the phase: a compound with $n = 0$ exists in the Y–Rh–Ge but not in the Y–Rh–Si system while compounds with n = 1,2 are formed when R = Y, T = Ir, M = Si but not when Si is replaced by Ge. However, when compounds are formed with both Si and Ge these crystallize with the same stacking mode. For the systems under consideration different stacking modes at the same stoichiometry are in fact only observed in some cases when Rh is replaced by Ir. The stacking of the Laves-type slabs in the Rh-containing compounds belonging to the ternary structure series changes from *r* (as in $MgCu_2$, rhombohedral branch) to *h* (as in $MgZn_2$, hexagonal branch) to *r* when the number of intermediate $CeCo_3B_2$-type slabs goes from 0 to 2 and the distance between subsequent Laves slabs increases. The corresponding sequence for the Y–Ir–Si system is –, *h*, *h*, while for the compounds belonging to the binary structure series the sequence *r*, *h*, – is observed for the Y–Rh system but *r*, *r*, – for the Y–Ir system (see Table 3). The symbol – means that no compound is formed.

In the case of Mg-containing Laves phases, where also more-complicated stacking sequences have been identified, the percentage of hexagonal stacking (as in $MgZn_2$) can be related with success to the valence-electron concentration (VEC) (Laves & Witte, 1936; Komura, Mitarai, Nakaue & Tsujimoto, 1972; Parthé, 1974; Komura & Kitano, 1977). To calculate the VEC, Mg is considered to have 2 valence electrons, Fe, Co and Ni 0, Cu and Ag 1, Zn 2 and Si 4 respectively. However, when Mg is replaced by lanthanide atoms the same relation does not hold. For example, inside the series of the 'isoelectronic' ROs_2 compounds a change in the stacking mode from cubic to hexagonal is observed between $PrOs_2$ and $NdOs_2$. The simple consideration of the number of valence electrons is not sufficient either when studying the stacking of the Laves-type slabs in the compounds listed in Table 3. For example, a calculation of the conventional VEC is of no help in the explanation of the different behaviour of Rh and Ir since both elements have the same number of outer *d* electrons.

Comparison of cell parameters

As compared with the compounds crystallizing with the $CaCu_5$ type an important contraction of the structure along the *c* axis is observed for all ternary compounds crystallizing with the $CeCo_3B_2$ type or one of its deformation variants. A similar, however less important, variation is noted when comparing the ternary Laves-type phases with the binary ones. In this way, for all compounds belonging to the two structure series containing ternary $CeCo_3B_2$ slabs the ratio C/a, where C is the average thickness of one slab, is significantly lower (0·67–0·71 for the compounds in Table 3) than the corresponding ratios calculated for the binary compounds (0·80–0·84). This contraction along the three- or sixfold axis allows for a closer contact between T and M atoms than between T atoms. Consideration of the variation of a and C among the members of the binary $R_{2+n}T_{4+5n}$ structure series in one of the binary systems in Table 3 shows that the average thickness of the slabs remains similar whereas a

decreases slightly when the fraction of $CaCu_5$-type slabs increases. Little variation is observed in the C/a ratio. The situation is different for the members of the ternary series $R_{2+n}T_{3+3n}M_{1+2n}$. In fact, as mentioned above, the compression of the structure along the c axis is larger for the $CeCo_3B_2$-type slabs than for the ternary Laves-type slabs. As expected, the average thickness of the slabs is smaller the higher the fraction of $CeCo_3B_2$-type slabs in the structure. The a parameter seems to be determined essentially by the $CeCo_3B_2$-type slab and varies little when going from 50 to 100% $CeCo_3B_2$-type slabs. As a consequence, C/a decreases when n increases.

We are indebted to the Département de Physique de la Matière Condensée, Université de Genève (Professor J. Muller), for letting us use some of their equipment, as well as to Mr A. Schweitzer and Mrs B. Künzler for technical assistance. This study was supported by the Swiss National Science Foundation under contract 2·035–0·86.

References

BODAK, O. I. (1971). *Visn. L'viv. Derzh. Univ. Ser. Khim.* **12**, 22–25.

BROWN, I. D. (1985). *Acta Cryst.* A**41**, 339.

CENZUAL, K., CHABOT, B. & PARTHÉ, E. (1987). *J. Solid State Chem.* **70**, 229–234.

CENZUAL, K., CHABOT, B. & PARTHÉ, E. (1988). *Acta Cryst.* C**44**, 221–226.

CORDIER, G., CZECH, E., OCHMANN, H. & SCHÄFER, H. (1984). *J. Less-Common Met.* **99**, 173–185.

CROMER, D. T. & LARSON, A. C. (1959). *Acta Cryst.* **12**, 855–859.

FRADIN, F. Y., RADOUSKY, H. B., ZALUZEC, N. J., KNAPP, G. S. & DOWNEY, J. W. (1982). *Mater. Res. Bull.* **17**, 427–434.

GHASSEM, H. & RAMAN, A. (1973*a*). *Z. Metallkd.* **64**, 197–199.

GHASSEM, H. & RAMAN, A. (1973*b*). *Metall. Trans.* **4**, 745–748.

HOVESTREYDT, E. (1983). *J. Appl. Cryst.* **16**, 651–653.

International Tables for X-ray Crystallography (1974). Vol. IV. Birmingham: Kynoch Press. (Present distributor D. Reidel, Dordrecht.)

KOMURA, Y. & KITANO, Y. (1977). *Acta Cryst.* B**33**, 2496–2501.

KOMURA, Y., MITARAI, M., NAKAUE, A. & TSUJIMOTO, S. (1972). *Acta Cryst.* B**28**, 976–978.

KRIKORIAN, N. H. (1971). *J. Less-Common Met.* **23**, 271–279.

KUZ'MA, YU. B. (1979). *Dopov. Akad. Nauk Ukr. RSR Ser. A*, pp. 146–151.

KUZ'MA, YU. B. & CHABAN, N. F. (1980). *Dokl. Akad. Nauk Ukr. SSR Ser. A*, pp. 88–91.

KUZ'MA, YU. B., KRIPYAKEVICH, P. I. & BILONIZHKO, N. S. (1969). *Dopov. Akad. Nauk Ukr. RSR Ser. A*, pp. 939–941.

LAVES, F. & WITTE, H. (1936). *Metallwirtschaft*, **15**, 840.

NORÉUS, D., ERIKSSON, L., GÖTHE, L. & WERNER, P.-E. (1985). *J. Less-Common Met.* **107**, 345–349.

PACCARD, L. & PACCARD, D. (1985). *J. Less-Common Met.* **109**, 229–232.

PACCARD, L., PACCARD, D., MOREAU, J. M. & GOMEZ-SAL, J. C. (1985). *J. Less. Common Met.* **107**, 291–294.

PARTHÉ, E. (1974). *In XXIV Congress of Pure and Applied Chemistry*, Vol. 3, pp. 139–158. London: Butterworth.

PARTHÉ, E. & CHABOT, B. (1984). In *Handbook on the Physics and Chemistry of Rare Earths*, edited by K. A. GSCHNEIDNER & L. EYRING, Vol. 6, ch. 48, pp. 113–334. Amsterdam: North-Holland.

PARTHÉ, E. & LEMAIRE, R. (1975). *Acta Cryst.* B**31**, 1879–1889.

RAMAN, A. & GHASSEM, H. (1973). *J. Less-Common Met.* **30**, 185–197.

STEWART, J. M., MACHIN, P. A., DICKINSON, C. W., AMMON, H. L., HECK, H. & FLACK, H. (1976). The *XRAY76* system. Tech. Rep. TR-446. Computer Science Center, Univ. of Maryland, College Park, Maryland, USA.

TEATUM, E., GSCHNEIDNER, K. JR & WABER, J. (1960). Cited in *The Crystal Chemistry and Physics of Metals and Alloys* (1972), by W. B. PEARSON, p. 151. New York: John Wiley.

VILLARS, P. & CALVERT, L. D. (1985). *Pearson's Handbook of Crystallographic Data for Intermetallic Phases*. Metals Park, OH: American Society for Metals.

WITTE, H. (1939). *Metallwirtschaft*, **18**, 459–463.

YVON, K., JEITSCHKO, W. & PARTHÉ, E. (1977). *J. Appl. Cryst.* **10**, 73–74.

Acta Cryst. (1988). C**44**, 405–409

Hexatellurium Octaselenium Hexakis(hexafluoroarsenate) Sulfur Dioxide

BY MICHAEL J. COLLINS, RONALD J. GILLESPIE AND JEFFERY F. SAWYER

Department of Chemistry, McMaster University, Hamilton, Ontario, Canada L8S 4M1

(*Received* 8 *July* 1987; *accepted* 26 *October* 1987)

Abstract. $(Te_6^{4+})(Se_8^{2+})(AsF_6^-)_6(SO_2)$, $M_r = 2594{\cdot}9$, triclinic, $P\bar{1}$, $a = 12{\cdot}407$ (4), $b = 12{\cdot}465$ (3), $c = 14{\cdot}109$ (5) Å, $\alpha = 96{\cdot}62$ (2), $\beta = 90{\cdot}49$ (3), $\gamma = 95{\cdot}13$ (2)°, $U = 2158$ (1) Å^3, $Z = 2$, $D_x = 3{\cdot}99$ g cm^{-3}, Mo $K\alpha$ radiation ($\lambda = 0{\cdot}71069$ Å), μ(Mo $K\alpha$) = 164·5 cm^{-1}, $F(000) = 2276$, $T = 298$ K, $R = 0{\cdot}063$ for 4896 reflections with $F > 4\sigma(F)$. The structure contains the previously known trigonal prismatic Te_6^{4+} cation and the *exo–endo* cyclic Se_8^{2+} cation. The anion–cation interactions in the structure are discussed.

Introduction. In attempting to prepare new mixed Te–Se cations by the oxidation of mixtures of tellurium and selenium with AsF_5 in SO_2 as solvent, we have obtained a new dark green crystalline compound which has been shown by X-ray crystallography to contain

0108-2701/88/030405-05$03.00